Binding modes of potential anti-prion phytochemicals to PrPC structures in silico

Sandesh Neupane
SANN Internatioanl College https://orcid.org/0000-0003-0677-8289
Jenisha Khadka
SANN International College
Sandesh Rayamajhi
SANN International College
Arti S. Pandey (arti.pandey69@gmail.com)
https://orcid.org/0000-0002-0262-5835

Research article

Keywords: anti-Prion, phytochemicals, terpenes, quinones, sterols, pharmacokinetics

Posted Date: October 25th, 2019

DOI: https://doi.org/10.21203/rs.2.16451/v1

Abstract

Background: Prion diseases involve the conversion of a normal, cell-surface glycoprotein (PrPC) into a misfolded pathogenic form (PrPSC). Cellular assays and in vivo experiments have identified various compounds with anti-prion activity which work through various mechanisms. Structures of PrPC have revealed the protein to occur in a swapped or non-swapped, monomeric or dimeric forms. Binding modes of known anti-prions is either not known, or has been determined with only the non-swapped structures of PrPC . In the current study medicinal phytochemicals from various databases have been docked with PrPC in silico to identify potential anti-prions in comparison with known anti-prion compounds to determine their binding modes and speculate possible mechanisms of inhibition of PrPC to PrPSC .

Results: Eleven new phytochemicals were identified based on their binding energies and pharmacokinetic properties. The binding sites and interactions of the known and new anti-prion compounds are similar, and differences in binding modes occur in structures with very subtle differences in side chain conformations. Binding of these compounds poses steric hindrance to neighbouring molecules. Residues shown to be associated with inhibition of PrPC to PrPSC conversion form interactions with most of the compounds.

Conclusions: The new compounds are mostly highly hydrophobic and are derivatives of terpenes, sterols and quinones. They might act as potent inhibitors of the PrPC to PrPSC conversion through a combination of steric hindrance and stabilization of structure through ionic/hydrophobic interactions. Their high binding energies coupled with identical binding sites as those of the known compounds, and their ability to cross the blood brain barrier makes these phytochemicals a promising group of compounds for further studies on prevention of PrPC to PrPSC .

Background

Prion diseases are fatal neurodegenerative diseases caused by conversion of a normal, cell-surface glycoprotein (PrP^{C}) into a misfolded pathogenic form (PrP^{Sc}), which causes a wide array of degenerative neurological disorders. [1]. The more stable PrP^{Sc} (also referred to as PrP^{res} for protease-resistance) denotes scrapie associated prion protein which are misfolded, beta-sheet-rich structures with low Gibbs free energy [2, 3].

To date no medication has been shown to halt or even slow prion or other neurodegenerative conditions [4]. All putative anti- Transmissible Spongiform Encephalopathy (anti TSE) drugs tested to date are prophylactic rather than therapeutic [5, 6]. Many anti-prion compounds like suramin, pentosanpolysulfate, amphotericin B, cyclodextrins, phenothiazine, statin[7], doxycycline, Congo red, rapamycin, dendritic polyamines, polyphenol, diphenylpyrazolebis-acridine, anti-histamine, and some anti-malarial agents including quinacrinemefloquine, etc.have

been reported to inhibit PrP^{Sc} formation or to reduce the level of PrP^{C} *in vitro*. However, they were not usable because of their toxicity and inability to cross the blood-brain barrier (BBB)[8].

High throughput virtual screening and structure-based drug design is cost effective and has speeded up the drug discovery process [9]. Many compounds identified through such *in silico* screening methods are under clinical trials as anti-prions or have become approved for therapeutic use [10, 11]. Compounds like GN8 (2-pyrrolidin-1- yl-N-[4-[4-(2-pyrrolidin-1-yl-acetylamino)-benzyl]-phenyl]-acetamide) [12], GJP49 (8-Methyl-7-{[2-(1-piperidinyl)ethyl]sulfanyl}-2,3-dihydro[1,4]dioxino[2,3-g]quinoline)[13] , and LD7 (Phenethyl Piperidines)[14] have been shown to stabilize PrP^{C} and prolong the survival of mice infected with prions. Recently, flavonoids baicalein and baicalin(baicalein 7-O-glucuronide), the active compounds from the North American traditional medicinal herb *Scutellaria lateriflora*, were found to reduce PrP^{Sc} accumulation in scrapie-infected cell cultures and cell-free conversion assays[15].

The science of ethno-botany has contributed to natural product research for the development of drug molecules or ethnobotanical leads. A wide range of Central Nervous System (CNS) active medicinal plants with resins and volatiles oils are used in different cultures to treat headaches, improve mood, alter perceptions, and to improve CNS health [16, 17]. In this study, we have integrated traditional ethnobotanical knowledge with *in silico* Computer Aided Drug Designing for the identification of potential plant derivative compounds that might inhibit the pathogenic conversion of PrP^{C} to PrP^{Sc}.

The normal globular domain of human PrP^{C}structure contains three α-helices comprising the residues 144–154, 173–194, and 200–228, and a short anti-parallel β-sheet comprising the residues128–131 and 161–164 [18]. The crystal structures of the human prion protein WT/M129 (1I4M) [18], , 4KML [19] and human prion protein variants WT/V129 (3HAK & 3HAF), D178N /M129 (3HEQ), and D178N/V129(3HJX) [20] have been determined at high resolution and have been shown to occur as swapped (1I4M and 3HAF) or un-swapped (3HEQ , 3HJX) dimers, non-swapped monomers (3HAK) and an ordered N terminus β sheet containing structure stabilized by a nano-molecule(4KML). Individual monomers of these structures were used for docking to identify high affinity compounds of which the ones meeting ADMET(absorption, distribution,

metabolism, elimination, toxicity) criteria were chosen for analysis of structural features determining the differences in their binding modes.

Results

Eleven new plant derivatives that can serve as potential inhibitors of PrP^C aggregation are listed in Table 1.All of the compounds are absorbed in the intestine and can cross the blood brain barrier, are non-toxic andnon carcinogenic. They do not inhibit renal organic anion transporters and show low Cytochrome P450 (CYP450) inhibitory promiscuity. Only RAU25 and BIO115 amongst the new compounds are inhibitors of CYP450 2C9, as is GJP49 from the known anti-prions.

Binding energies (BE): Compounds binding to the prion protein through pi-alkyl/alkyl/pi-sigma interactions bind more strongly compared to those that bind through hydrogen bonding. The known anti-prion compounds bind to the swapped structures (mean = 7.31 kcal/mol) more strongly than to the non- swapped structures (mean = 6.59 Kcal/mol). The new identified compounds also bind stronger to the swapped (mean = 9.125 kcal/mol) than to the non-swapped structures (mean = 7.728 kcal/mol)(Supplement S1). The strongest BE is that of the compound EA150 to HAF (-10.8 kcal/mol).

Table 1: List of newly identified plant derivatives, their sources, chemical names, modes of binding and binding energies with the swapped and non-swapped crystal structures. BE-Binding energy, R-alkyl, HB-hydrogen bond.

Comp.	Plant	Chemical name	BE Kcal/mol	Interactions	Regions
3HAF (WT/V129) (Swapped)					
ILE2	*Ilex paraguariensis*	βamyrin	-8.6	Pro 158 (R), Ile 184(R),Tyr157(π-R)	α1- α2, α2, α1- α 2
CEN39	*Centellaasiatica*	campesterol	-8.3	Tyr149(π-σ),Tyr145(π -R), Tyr149(π -R), Tyr157(π -R)	N-ter, α 1- α 2
PTY55	*Ptychopetalumolacoides*	β -sitostenone	-8.4	Pro158 (π -R), Tyr157(π -R), Phe141(π -R),Tyr149(π -R)	α1-α 2, N-ter, α1
EA150	*African medicinal plant*	(9β,13α)13,28Epoxyoleanane-3,22-dione	-10.8	Pro137(π -R),Tyr157(π -R), Tyr150(π -R), Tyr149(π -R)	N-ter , α 1-α 2, α 1
I4M (WT/M129)(Swapped)					
PTY55	*Ptychopetalumolacoides*	β sitostenone	-8.7	Pro158(R), Tyr157(π -R), Phe141(π -R)	α 1-α 2, N-ter
CEN39	*Centellaasiatica*	Campesterol	-8.4	Phe141(π -R), Pro158(R),Tyr157(π -σ)	N-ter, α 1-α 2
HAK (WT/V129) (Non-swapped)					
CEN36	*Centellaasiatica*	Asiatic Acid	-7.4	His187(π-Alkyl),Tyr162 (HB), Thr183(HB)	α 2, β 2
RAU31	*Rauvolfiaserpentina*	Rescinnamine	-7.4	Lys194(H-bond),Thr183 (C-H), Tyr162 (HB),Gln160 (C-H), His155(C-H)	α 2, β 2, α 1- α 2
BNP 8864	*Sophoravelutina*	Olean-12-en-3-ol	-8.6	His187(Alkyl), His187(Alkyl) Pro158(Alkyl)	α1- α2, α 2
BNP 2069	*Glyptopetalumsclerocarpum*	22-Hydroxytingenone	-8.2	His187(π -R), Tyr162(π -R), His155(HB),Arg136(HB)	α 2, β 2, α 1-α 2, N-ter
HEQ (D178N/M129)(Non-swapped)					
RAU25	*Rauvolfiaserpentina*	Ajmalicine	-7.8	Thr191(HB), Lys194(HB), Pro158(π -σ)	α 2, α 1-α 2
HJX(D178N/V129(Non-swapped)					
EPH18	*Ephedra sinica*	Ellagic acid	-7.3	Pro158(π -R), His155(HB), Tyr157(HB), Thr191(HB)	α 1- α 2, α 2
Bio115	*Handroanthusimpetiginosus*	atovaquone	-7.4	His155(HB), Tyr157(HB), Asn159(HB)	α 1- α 2
KML(WT-M129 in complex with nanobody Nb484), with Nb484 deleted(Non-swapped)					
RAU31	*Rauvolfiaserpentina*	Rescinnamine	-7.1	Tyr163(HB),Asp167(HB),Pro165(π -R), Ala224(HB),Glu221(HB)	β2, α1-α2, C-ter
Bio115	*Handroanthusimpetiginosus*	atovaquone	-6.6	Glu207(HB), Thr188(π -σ), Val203(π -R)	α3, α 2

Binding regions: The regions where known as well as potential anti-prion compounds bind are shown in Fig. 1B for the three types of structures available. All of these compounds bind to the α1-α2 or the α2-α3 loops or to both (Fig. 1A), with a few interactions with residues of the C-terminii of α1 and α2. Subunits of swapped dimers have a very small region of binding and very few ionic interactions while binding to non- swapped PrP^C also extends towards the N-terminus of α3 and C-terminus of α2 including the α2-α3 hinge loop residues. Binding to the structure

with ordered β sheet N-terminus residues uniquely shows binding throughout α2 and the C-terminus of α3.

Binding sites :Swapped structures

The swapped dimers I4M and HAF structurally align with root mean square deviation (r.m.s.d) of 0.294.The known anti-prion compoundsinteract with the same regions of the prion protein structures as the new compounds, with the exception of LD7, which forms all interactions with α2 (Table 1, Fig. 1A). The number of ionic interactions between swapped monomers and new compounds are very few compared to those of the known compounds, which interact extensively with all helices and loops. In all cases, the site of binding of these compounds is through hydrophobic residues on α2 which form the interface of association withα3 of another monomer to form the dimer. Steric clashes of the bound compounds become apparent with α3 when the dimer is created from the compound bound monomers (Fig.2A). Monomers of both swapped structures I4M and HAFbind CEN39 and PTY55 in the same regions. However, the known anti-prion compounds LD7 and GJP 49 bind with similar binding energies to different sites on I4M and HAF: to a crevice formed by the switch loop and the C-terminii of α1 and α2 in I4M versus a surface binding between α1 and α2 in HAF (Fig. 3).

Binding sites : Non-swapped structures

Binding to non-swapped monomer occurs mostly to residues of the C-termini of α1 and α2, with some interactions with the α2-α3 switch region (Fig. 1A and 1B). HAK presents a “tighter” structure as residues 190-194 continue asα2 helix, whereas in other non-swapped structures, they form a loop. HJX which presents a more disordered and open α2-α3 loop allows molecules to extend into the space created by a loosening of this loop. However, only the known anti-prions GJP49 and GN8 are able tooccupy this space.Rau31 binds to different sites on HAK and KML which superimpose with r.m.s.d 0.655. The site of binding of RAU31 in KML involves residues of α3 C-terminus and α2 N-terminus(Fig. 1A, Fig. 4B). However, no residue from the N-terminus β sheets is seen to interact with the compound. Bio115 binds to KML as well as HJX (r.m.s.d 1.367) at different sites : to the hinge loop region towards the flip side of α1 in KML whereas in HJX , it binds to the front of the hinge loop facing α1, along with all other compounds. As with other non-swapped structures compared with HJX, the hinge loop region is more organized in KML and tighter, with Thr 190 to Lys 194 a part of α2 in the latter.

Binding of compounds in all structures results in steric clashes either with the partner monomer or with a crystallographic symmetry related molecule (Fig. 2B). BIO115 in HJX sterically clashes with another BIO115 as well as its α2-α3 loop on its partner monomer (Fig. 2B(c)). Ligands bound to HAK sterically clash with residues of three different symmetry related monomers (Fig. 2B(a)). Steric clashes in HEQ occur only between known anti-prions in the symmetry related dimers (Fig.2B(d)). RAU31 in KML sterically clashes with residues form a symmetry related molecule (Fig. 2B(c)).

β sheet regions: The residues 188-195 are involved in hydrogen bonding with the same region of the other monomer to form a β sheet in both swapped structures.The known anti-prions LD7 and GJP49 sterically clash with the Lys194 side chain of the partner monomer in this region in swapped structures .No interactions occur in either type of structures with residues of the β-strand formed by residues 128-131. All new compounds binding to the non-swapped structures interact with one or the other of Tyr162, Tyr 163 , Lys194, Thr188 and Thr191, which are constituents of β strands in either swapped or non-swapped structures.

Discussion

Binding energies: Compounds listed in Table 1 as potential anti-prion compounds bind with comparable or higher binding energies as those of the known anti-prion compounds. The binding sites of the new found compounds are also the same as the known anti-prion compounds LD7, GJP 49 and GN8, with minor differences in residue specific interactions. None of the new compounds have an extended structure as GN8 or LD7, which can form interactions with more residues and hence, can block more surface area of the protein to prevent association. The new compounds show high binding energy and might not be able to dissociate easily from the protein once they are bound, acting as potential inhibitors by steric hindrance of other prion protein molecules as depicted in Fig.2A and Fig. 2B.However, high binding energies through docking do not always correlate with binding to PrP^{C} *in vivo*[33] , and sites to which binding occurs on the proteinalso play an important role in determining the conversion to PrP^{Sc} .

Binding sites (Swapped structures)

Binding of all known and potential anti-prion compounds in the same region of I4M and HAF is expected, as they are very similar except for the Met and Val respectively at position 129. The binding of LD7 and GJP49 to the two structures at different sites(Fig. 3) highlights the effect of

subtle changes in side chain conformations irrespective of the binding energies which are around 7Kcal/mole (Supplementary Materials S1, Table 1).The side chain conformations of Asn 197 and Glu196 are different in the two structures (Fig. 3) such that Glu196 side chain in HAF extends into the cleft that is formed by residues of the switch region.Similarly, binding of CEN39 to both I4M and HAF is in the same site, but the molecule is flipped to bring the OH group to the opposite end. Although there are slight differences in the side chain conformations of close by residues 140 -146 in the two structures, these are unlikely to affect CEN39 binding and both orientations might be possible in a swapped structure.This is reflected in the similar binding energies of CEN39 to both structures (Table 1).

The new compounds identified are highly hydrophobic and bind mainly through hydrophobic alkyl and pi-alkyl interactions to residues of α1 (Table 1).It has been proposed that when α1 is caused to either unravel or be pushed away from the α2- α3 subdomain, misfolding is accelerated. [34]Tight binding of compounds to residues of α1can help stabilize it and prevent its movement. Inhibition of PrP^{C} to PrP^{Sc} conversion by potential anti-prion compounds differs with cell types and correlates with interactions with Asn159 and Glu196. [33]The ionic interactions between the new compounds and both the swapped structures are very few and encompass Glu146, Pro158, Asn159 and Gln160, while their hydrophobic regions extend along the protein surface.Dimerization of PrP^{C} has been found to be the rate limiting step during oligomerization and misfolding.[34]As these compounds occupy the region that is filled in by the swapped α3 of another monomer to form a dimer, the prevention of association of α3 of one monomer with α1 of the other can contribute to the inhibitory activity of these compounds towards PrP^{C} to PrP^{Sc} conversion.

Binding sites: non-swapped structures

There is a shift in binding of molecules from mainly the hinge loop in HJX towards mostly surface binding to HAK between α1 and α2. The non-swapped structures differ from each other in rotation of α2 away from the N-terminus of α3. There are accompanying unraveling of the C-termini residues of α2 comprising Thr191 – Lys194 , which form an additional helix fold in HAK, are somewhat ordered into a helix in HEQ and completely disordered in HJX. The energy minimized structure of this loop in HJX shows Lys194 side chain extended towards the solvent while Asn197 extends towards the protein interior. In the other two structures, Lys 194 turns

inwards while Asn 197 extends into the solvent away from the protein surface. LD7 binds to the surface opposite to where the rest of the compounds bind in HAK which also shows a strong (2.8A) interaction between imidazole ring of His 187 with the main chain carbonyl oxygen of Arg 156. HAK and HJX show larger distances between these residues as shown in Fig. 4A. It is likely that the access to residues in the loop region is reduced due to residues interacting with each other as in HAK.

The conformation of the side chain of Met 166 is flipped in KML compared to HAK so that it is turned towards the C-terminus of the protein. However, in HAK, the Met 166 side chain is turned towards the exterior of the protein and exposed to solvent(Fig. 4B). Similarly, the side chain of Tyr 169 in KML turns towards the interior of the protein, while in HAK it faces the solvent. Although the short helix in this region ranges from Pro165 to Tyr 169, the side chains of the residues comprising this region are arranged in different conformations which probably cause the difference in binding of RAU 31 to different regions of these two structures. Residues Tyr162 to Asn171 in KML constitute a loop-β-helix-loop secondary structure domain that interacts closely with the N-terminus β sheet as well as the stabilizing nano molecule co-crystallized with PrP^{C}.The R164-S170 loop has been suggested to allow transmission of conformational information to influence intermolecular β sheet formation. [35]RAU31 interacts with the small β sheet in both HAK as well as KML and could help disrupt the intermolecular β sheet structures comprising Tyr162,Tyr163 and Met/Val129,Ile 130 seen in the D178N mutants. [35] RAU31 also forms ionic interactions with residues Arg 220, Glu221 and Ala224of C-terminusα3 in KML. The known anti-malarial drug quinacrine, which has also been shown to be an inhibitor of PrP^{Sc} formation has been shown to bind to Tyr225, Tyr 226 and Gln 227 of α3 in PrP. [36]Anchorless PrP^{C} truncated at the C terminus are more prone to PrP^{Sc} formation at low pH[37] presumably due to a decrease in intra-molecular interactions in the C-terminus residues, so that they are available for inter-molecular interactions. Following this theory, RAU31 binding to residues of the C-terminus can also decrease the availability of ionic interactions for another PrP monomer, reducing the chances of dimerization.RAU31 hence might be able to act by stabilizing the N-and C- termini, interacting withAsn159 ,residues of the switch region and the residues of the intermolecular β sheet, to inhibit PrP^{C} to PrP^{Sc}conversion.

Based upon *ex vivo* and *in vivo* treatment experiments [38], anti-prion compounds have been proposed to act through specific or non-specific conformational stabilization, reduction of PrP^{C} through precipitation and interaction with molecules other than PrP^{C}.[35] Inhibition of PrP^{C} to PrP^{Sc}conversion by potential anti-prion compounds differs with cell types and correlates with interactions with Asn159 and Glu196.[33] Compounds binding to both swapped and non swapped structures show ionic interactions with Asn 159, none interact with Glu196. But many of the new found compounds strongly interact with Pro158 and Asn 197. It can be assumed that the binding of compounds to regions of PrP^{C} determines inhibition rather than binding to specific amino acids and that binding to residues 158 and 197 will be as effective for inhibition as binding to residues 159 and 196. Moreover, binding to Asn197 is possible only in the non- swapped forms where it is fully exposed. Asn197 is a site of glycosylation of PrP^{C}[39]and its blocking by an inhibitor can influence both the movement of the hinge region to prevent α3 from swapping as well as by mimicking an *in vivo* glycan as seen in PEGylated (Polyethyleneglycol)PrP at 181 and 197 that inhibit PrP^{Sc} formation. [40]

A number of studies have shown changes in conformation of PrP^{C} resulting from lowering of pH and/or chemical denaturants and that these altered conformation intermediates display one or the other characteristics of PrP^{Sc}. [41] A lowering of pH causes marked chemical shifts in the C-termini of α1 and α2; specifically Asn186, His187, Thr188, Thr192, Lys194 and Glu196 of α2 and His155, Arg156 and Asn159 of α1 as a result of protonation of His187 and His155 . [41] The protonation of His187 favors PrP^{Sc} like conformation while de-protonation favors native PrP^{C}[41]The known anti-prion compounds LD7,GJP49 and GN8 bind to one or the other of these residues. All new compounds that bind to the non-swapped forms interact either with His155 or His187. Involvement of these histidines in interactions with the compounds might discourage their protonation and hence also the development into an altered conformation intermediate. A low pH treatment of recombinant mouse PrP^{C} is also accompanied by increased solvent exposure of tyrosine side chains in addition to a 25 times higher recognition of $PrP^{Sc}$by Tyr-Tyr-Arg antibodiescompared to PrP^{C}. [42] The Tyr-Tyr-Arg motif occurs in two regions res.149-151 and res. 162-164 in the prion protein. The new compounds stack with one or the other of these tyrosinesand alsoform non-polar interactions with Pro 158 in the swapped monomers. Stacking of

rings of the terpenes and sterols can be visualized as tightening hydrophobic interactions and preventing the alteration in the side chain conformations of tyrosines, and by extension of the PrP^{Sc} forming intermediates. Flanking proline residues in prion proteins have also been proposed to have a containment role and confine the β sheet within a specific length. [43] Hydrophobic interactions of compounds with prolines will reinforce its position and hence its role in prevention of lengthening of the β sheet.

Potential bioactive anti-prion compounds

All new compounds are either tetra- or pentacyclic terpenoids, sterols and naphthoquinones. Most of these have been shown to be utilized for various medicinal purposes in humans. All of them are able to cross the blood brain barrier, bind very strongly to PrP^{C} and can prove to be potent anti-prion compounds. Different compounds bind to different forms, the swapped dimer being the least amenable to binding. The presence of the N-terminus β sheet structure might offer more binding sites for stabilization of the soluble monomeric form and prevention of dimerization.

Rau25 or Ajmalicine is an α1 adrenergic receptor antagonist used as a anti-hypertensive drug[44]. It is a heteropentacyclicmonoterpenoid indole alkaloid and methyl ester found in the root or bark of several plant species including Rauwolfia spp, *Catharanthusrosea*etc[45].RAU31 orRescinnamine , is a heteropentacylicvinca alkaloid also derived from *Rauwolfia serpentina* and other species of Rauwolfia [46] used as an antihypertensive drug and an angiotensin converting enzyme inhibitor.

CEN36 (Asiatic acid) and CEN39 (campesterol)are a triterpene and sterol derivative respectively from *Centellaasiatica*. *Centellaasiatica* contains a variety of saponins of which asiaticoside, an asiatic acid derivative, has been suggested to exert a therapeutic effect in Alzheimer's disease. [47]Asiatic acid has also been found to be neuroprotective in a mouse model of focal cerebral ischemia [48]. *Centellaasiatica* synthesizes saponins (triterpenes) including asiatic acid and sterols including campesterol from mevalonic acid via the isoprenoid pathway. [49]Campesterol has been demonstrated to be able to cross the blood brain barrier in mice.[50] There is no flux of lipoprotein bound cholesterol across the blood brain barrier, but the presence of an alkyl group

on the 24-position of cholesterol side chain (campesterol) results in a markedly increased ability to cross the intact blood brain barrier.[51]

BNP2069(22 hydroxytingenone or tingenin B), a pentacyclic quinine methide triterpenoid compound has been found to possess antibacterial, antiparasitic and anticancer activities.[52] BNP8864 and ILE2 are different representations of olean-12 en-3-ol or β amyrin, a very commonly occurring pentacyclic triterpenoid that is oleanane substituted at the β position by a hydroxyl group, with a double bond between C12 and C13 and is found in many higher plant species.[53]β amyrin has been found to ameliorate the cognitive impairment induced by hypocholinergic neurotransmission, as is seen in Alzheimer's disease, via the activation of ERK as well as GSK-3 β signaling.[54]

PTY55 β sitostenone (Stigmast-4en-3-one) is a steroid derivative present in many plant species. β sitosterone and its corresponding alcohol β sitosterol from *Anacardiumoccidentale* (cashew) have been shown to have hypoglycemic activity demonstrated through an intravenous injection in healthy dogs.[55]EPH18 or ellagic acid is a natural polyphenolheterotetracyclic antioxidant derived from gallic acid, that occurs in numerous fruits and vegetables, especially in black raspberries and pomegranate juice. Ellagic acid has been found to exhibit antioxidant and anticarcinogenic properties including inhibition of tumor formation and growth both *in vitro* and *in vivo*.[56][57] Ellagic acid possesses potent neuroprotective effects through its free radical scavenging properties, iron chelation, activation of different cell signaling pathways and mitigation of mitochondrial dysfunction. [58]

Bio115 or atovaquone is a synthetic derivative of lapachol from *Tabebuia* species (Bignoniaceae). Atovaquone is an anti-malarial drug that inhibits the electron transport chain by binding to the quinol oxidation site of cytochrome bc1 complex.[59]EA150 is a compound from the natural product library of African medicinal plants [60]. There is not much information about this compound and its utility in medicine, except for its listing in the ZINC database. [61]It is a derivative of the pentacyclic triterpenoid oleanane.[62]

Conclusions

Thenew found compounds are derivatives of terpenes, sterols and quinones, and bind to the same regions of PrP as the known anti-prion compounds. The conformation of PrP^{C} to which these compounds bind differ and their mechanism of action may involve multiple effects ranging from a steric hindrance of association of monomers, blocking of the swapping of α 3 towardsα2, stabilizing the switch region between α2 and α3 , preventing protonation of histidines and reducing exposure of tyrosines to the solvent. As these compounds cross the blood brain barrier and are in use for medicinal purposes for various conditions, they form an attractive group of compounds to be considered for prevention of PrP^{C} to PrP^{Sc} conversion in isolation or in combination with each other. These compounds are an attractive group of phytochemicals to be considered for in vivo or cell culture studies as inhibitors of PrP^{C} to PrP^{Sc} conversion.

Methods

The plants, which are traditionally used to treat different neurodegenerative diseases, were listed by searching the dendrimer based drug delivery system [21]and PubMed Central focusingon plants known to have Central Nervous System (CNS) stimulant activity.

Construction of phytochemicals database

The bioactive constituents of these plants (phytochemicals) and their derivatives were searched for in the literature and structure databases including Pubmed, PubChem, Dr. Duke Phytochemical and Ethnobotanical databases, and Traditional Chinese Medicine Database System. The 3D structures of these phytochemicals/bioactivesweredownloaded from PubChem [22],eMolecules (www.emolecules.com) and ChemSpider[23]. Structures that were not available were created using ACD/Labs 2016 Freeware, v14.00, [24].Thus, an in-house database of 207 structures of phytochemicals known to act on the CNS was constructed.

The library was expanded to a total of 2550 molecules with additional molecules from different databases such as AfroDB[25] containing 954 potent natural products from African medicinal plants, $NuBBE_{DB}$[26] containing 643 bioactives from biodiversity of Atlantic forest, Brazil and IBScreenBioactives (http://www.ibscreen.com) containing 746 biologically active compounds, were downloaded from ZINC databases [27].An energy minimization was done for all molecules using universal force fields (UFF) from OpenBabel[28, 29], before docking to protein structures.

Target protein and Binding pocket preparation

The high resolutions crystal structures of human prion protein PrP^C with PDB (Protein Data Bank) accession code 3HAK, 3HAF, 3HEQ, 1I4M, 4KML and 3HJX were downloaded from the PDB.The water molecules were deleted from all of the six structures,missing amino acids in the 3HEQ and 3HJXwere added and the nano-molecule from the 4KML was removed using Accelrys's Discovery Studio Visualiser v16.1.0.153350. (DassaultSystèmes BIOVIA, BIOVIA Workbook, Release 2017). Energy minimization of the added residues for 3HEQ and 3HJX was done using chimera-1.13.1[30]. The co-ordinates of the nanomolecule that co-crystallized with PrP^C in 4KML were removed, and only the PrP^C coordinates were used for docking. The PDB IDs of the structures in the text have been mentioned without the preceding digits and the helices and sheets are mentioned as α and β respectively.

In-silico virtual screening

Docking was done in AutoDock Vina within open source software PyRx –Python Prescription 0.8 [31]. The Lamarckian Genetic Search Algorithm with default parameters were used in automated docking simulation. The search region cubic space encompassed the entire protein and the grid box dimension for respective protein structures (Supplement S2): only monomers (swapped or non-swapped) were included in the docking. The compounds of the in-house database along with compounds shown to have anti-prionic activity, namely GJP49, GN8, LD7were also docked against the human PrP^C protein as controls.

Pharmacokinetics and binding mode

The drug-likeness was evaluated, based on 'rule of 5' (Ro5), developed by Lipinski et al. [32] predicted with the online tool PreADMET (http://preadmet.bmdrc.org).The pharmacokinetic properties of potential anti-prion compounds in the human body, including their absorption, distribution, metabolism, blood brain barrier penetration and excretion as well as Toxicity were predicted using AdmetSAR (http://lmmd.ecust.edu.cn/admetsar1). Compounds with binding energies comparable to or higher than the known anti-prion compounds and satisfying the

ADMET criteria were selected for analysis of interactions, site of fit and distances using Accelrys's Discovery Studio Visualiser v16.1.0.153350.

Abbreviations

ADMET: absorption, distribution, metabolism, elimination, toxicity

BBB: Blood-brain barrier

BE: Binding Energies

CNS: Central Nervous System

PEG: polyethyleneglycol

PrP: Prion Protein

PrP^{C}: Cellular prion protein

PrP^{res}: Protease-resistant prion protein

PrP^{Sc}: Pathogenic scrapie prion

r.m.s.d.: root mean square deviation

TSE: Transmissible Spongiform Encephalopathy

UFF: Universal force fields

BIO115: atovaquone

BNP2069: 22 - Hydroxytingenone

BNP8864: Olean-12-en-3-ol

CEN36: Asiatic acid

CEN39: Campesterol

EA150: (9β 13 α) 13,2 8-Epoxyoleanane-3,22 dione

EPH18: Ellagic acid

ILE2: β-amyrin

PTY55: β-sitostenone

RAU 31: Rescinnamine

RAU25: Ajmalicine

Declarations

Ethics approval and consent to participate

Not applicable

Consent for publication

Not applicable

Availability of data and materials

The datasets used and/or analyzed during the current study are available from the corresponding author on request.

Competing interests

The authors declare that they have no competing interests.

Funding

Not applicable

Authors' contributions

SN built the in house library of phytochemicals, performed autodocking, and contributed to manuscript writing. JK and SR contributed to creation of database . ASP planned and supervised the docking, carried out structural analysis and contributed to manuscript writing. All authors have read and approved the final manuscript.

Acknowledgements

Not applicable

Authors' information

Not applicable

References

1. Prusiner SB. Nobel Lecture: Prions. Proceedings of the National Academy of Sciences. 1998;95:13363–83.
2. Kupfer L, Hinrichs W, Groschup MH. Prion protein misfolding. Current molecular medicine. 2009;9:826–35.
3. Yamamoto N, Kuwata K. Regulating the conformation of prion protein through ligand binding. Journal of Physical Chemistry B. 2009;113:12853–6.
4. Aguzzi A, Nuvolone M, Zhu C. The immunobiology of prion diseases. Nature Reviews Immunology. 2013;13:888–902.
5. Diaz-Espinoza R, Morales R, Concha-Marambio L, Moreno-Gonzalez I, Moda F, Soto C. Treatment with a non-toxic, self-replicating anti-prion delays or prevents prion disease in vivo. Molecular Psychiatry. 2017; April 2016:1–12.
6. Cashman NR, Caughey B. Prion diseases - Close to effective therapy? Nature Reviews Drug Discovery. 2004;3:874–84.
7. Kocisko DA, Baron GS, Rubenstein R, Chen J, Kuizon S, Caughey B. New inhibitors of scrapie-associated prion protein formation in a library of 2000 drugs and natural products. Journal of virology. 2003;77:10288–94.
8. Ishibashi D, Nakagaki T, Ishikawa T, Atarashi R, Watanabe K, Cruz FA, et al. Structure-Based Drug Discovery for Prion Disease Using a Novel Binding Simulation. EBioMedicine. 2016;9:238–49.
9. Baldi A. Computational approaches for drug design and discovery: An overview. Systematic Reviews in Pharmacy. 2010;1:99–105.
10. Singh DB. Success, Limitation and Future of Computer Aided Drug Designing. Translational Medicine. 2014;04.
11. Talele T, Khedkar S, Rigby A. Successful Applications of Computer Aided Drug Discovery: Moving Drugs from Concept to the Clinic. Current Topics in Medicinal Chemistry.

2010;10:127–41.

12. Kuwata K, Nishida N, Matsumoto T, Kamatari YO, Hosokawa-Muto J, Kodama K, et al. Hot spots in prion protein for pathogenic conversion. Proceedings of the National Academy of Sciences of the United States of America. 2007;104:11921–6.
13. Hosokawa-Muto J, Kamatari YO, Nakamura HK, Kuwata K. Variety of antiprion compounds discovered through an in silico screen based on cellular-form prion protein structure: Correlation between antiprion activity and binding affinity. Antimicrobial Agents and Chemotherapy. 2009;53:765–71.
14. Imberdis T, Heeres JT, Yueh H, Fang C, Zhen J, Rich CB, et al. Identification of anti-prion compounds using a novel cellular assay. Journal of Biological Chemistry. 2016;291:26164–76.
15. Eiden M, Leidel F, Strohmeier B, Fast C, Groschup MH. A medicinal herb Scutellaria lateriflora inhibits PrP replication in vitro and delays the onset of prion disease in mice. Frontiers in Psychiatry. 2012;3 FEB:1–8.
16. Rubia K, Alegria A, Brinson H. Imaging the ADHD brain : medication effects and clinical translation. Expert Review of Neurotherapeutics. 2014;14:519–38.
17. Mendes FR, Negri G, Duarte-Almeida JM, Tabach R, Carlini EA. The Action of Plants and their Constituents on the Central Nervous System. In: Plant Bioactives and Drug Discovery: Principles, Practice, and Perspectives. 2012. p. 161–204.
18. Knaus KJ, Morillas M, Swietnicki W, Malone M, Surewicz WK, Yee VC. Crystal structure of the human prion protein reveals a mechanism for oligomerization. Nature Structural Biology. 2001;8:770–4.
19. Abskharon RNN, Giachin G, Wohlkonig A, Soror SH, Pardon E, Legname G, et al. Probing the N-terminal β-sheet conversion in the crystal structure of the human prion protein bound to a nanobody. Journal of the American Chemical Society. 2014;136:937–44.
20. Lee S, Antony L, Hartmann R, Knaus KJ, Surewicz K, Surewicz WK, et al. Conformational diversity in prion protein variants influences intermolecular ??-sheet formation. EMBO Journal. 2010;29:251–62.
21. Wang B, Editor S. Wiley Series in Drug Discovery and Development. Dendrimer-Based Drug Delivery Systems. 2012;:515–6.
22. Kim S, Thiessen PA, Bolton EE, Chen J, Fu G, Gindulyte A, et al. PubChem substance and compound databases. Nucleic Acids Research. 2016;44:D1202–13.
23. Pence HE, Williams A. Chemspider: An online chemical information resource. Journal of Chemical Education. 2010;87:1123–4.
24. Li Z, Wan H, Shi Y, Ouyang P. Personal experience with four kinds of chemical structure drawing software: Review on chemdraw, chemwindow, ISIS/draw, and chemsketch. Journal of Chemical Information and Computer Sciences. 2004;44:1886–90.
25. Ntie-Kang F, Zofou D, Babiaka SB, Meudom R, Scharfe M, Lifongo LL, et al. AfroDb: A Select Highly Potent and Diverse Natural Product Library from African Medicinal Plants. PLoS ONE. 2013;8:e78085.

26. Valli M, Dos Santos RN, Figueira LD, Nakajima CH, Castro-Gamboa I, Andricopulo AD, et al. Development of a natural products database from the biodiversity of Brazil. Journal of Natural Products. 2013;76:439–44.
27. Sterling T, Irwin JJ. ZINC 15 - Ligand Discovery for Everyone. Journal of Chemical Information and Modeling. 2015;55:2324–37.
28. O'Boyle NM, Banck M, James CA, Morley C, Vandermeersch T, Hutchison GR. Open Babel: An Open chemical toolbox. Journal of Cheminformatics. 2011;3:1–14.
29. Dallakyan S. Small-Molecule Library Screening by Docking with PyRx. 2015;1263 January 2015.
30. Pettersen EF, Goddard TD, Huang CC, Couch GS, Greenblatt DM, Meng EC, et al. UCSF Chimera - A visualization system for exploratory research and analysis. Journal of Computational Chemistry. 2004;25:1605–12.
31. Trott O, Olson A. AutoDock Vina: improving the speed and accuracy of docking with a new scoring function, efficient optimization and multithreading. Journal of Computational Chemistry. 2010;31:455–61.
32. Lipinski CA, Lombardo F, Dominy BW, Feeney PJ. Experimental and Computational Approaches to Estimate Solubility and Permeability in Drug Discovery and Develop ment Settings. Advanced Drug Delivery Reviews. 1997;23:3–25.
33. Hyeon JW, Choi J, Kim SY, Govindaraj RG, Hwang KJ, Lee YS, et al. Discovery of Novel Anti-prion Compounds Using In Silico and In Vitro Approaches. Scientific Reports. 2015;5:14944.
34. Sabareesan AT, Udgaonkar JB. Pathogenic Mutations within the Disordered Palindromic Region of the Prion Protein Induce Structure Therein and Accelerate the Formation of Misfolded Oligomers. Journal of Molecular Biology. 2016;428:3935–47.
35. Lee S, Antony L, Hartmann R, Knaus KJ, Surewicz K, Surewicz WK, et al. Conformational diversity in prion protein variants influences intermolecular ??-sheet formation. EMBO Journal. 2010;29:251–262.
36. Vogtherr M, Grimme S, Elshorst B, Jacobs DM, Fiebig K, Griesinger C, et al. Antimalarial Drug Quinacrine Binds to C-Terminal Helix of Cellular Prion Protein. J Med Chem. 2003;46:3563–4.
37. Kovač V, Hafner-Bratkovič I, Čurin Šerbec V. Anchorless forms of prion protein – Impact of truncation on structure destabilization and prion protein conversion. Biochemical and Biophysical Research Communications. 2016;481:1–6.
38. Kamatari YO, Hayano Y, Yamaguchi KI, Hosokawa-Muto J, Kuwata K. Characterizing antiprion compounds based on their binding properties to prion proteins: Implications as medical chaperones. Protein Science. 2013;22:22–34.
39. Aguzzi A, Baumann F, Bremer J. The Prion's Elusive Reason for Being. Annu Rev Neurosci. 2008;31:439–77.
40. Araman C, Thompson RE, Wang S, Hackl S, Payne RJ, Becker CFW. Semisynthetic prion protein (PrP) variants carrying glycan mimics at position 181 and 197 do not form fibrils

†Electronic supplementary information (ESI) available. See DOI: 10.1039/c7sc02719b Click here for additional data file. Chem Sci. 2017;8:6626–32.

41. Hosszu LLP, Tattum MH, Jones S, Trevitt CR, Wells MA, Waltho JP, et al. The H187R mutation of the human prion protein induces conversion of recombinant prion protein to the PrP(Sc)-like form. Biochemistry. 2010;49:8729–38.
42. Paramithiotis E, Pinard M, Lawton T, LaBoissiere S, Leathers VL, Zou W-Q, et al. A prion protein epitope selective for the pathologically misfolded conformation. Nat Med. 2003;9:893–9.
43. Shamsir MS, Dalby AR. β-Sheet Containment by Flanking Prolines: Molecular Dynamic Simulations of the Inhibition of β-Sheet Elongation by Proline Residues in Human Prion Protein. Biophysical Journal. 2007;92:2080–9.
44. ajmalicine (CHEBI:2524). https://www.ebi.ac.uk/chebi/searchId.do;?chebiId=CHEBI:2524. Accessed 23 May 2019.
45. Chopra R, Nayar S, Chopra I. Full text of “Glossary Of Indian Medicinal Plants (1956).” New Delhi, India: Council of Scientific and Industrial Research; 1956. https://archive.org/stream/in.ernet.dli.2015.507107/2015.507107.Glossary-Of_djvu.txt. Accessed 23 May 2019.
46. Fife R, Maclaurin JC, Wright JH. Rescinnamine in Treatment of Hypertension in Hospital Clinic and in General Practice. Br Med J. 1960;2:1848–50.
47. Mook-Jung I, Shin JE, Yun SH, Huh K, Koh JY, Park HK, et al. Protective effects of asiaticoside derivatives against beta-amyloid neurotoxicity. J Neurosci Res. 1999;58:417–25.
48. Krishnamurthy RG, Senut M-C, Zemke D, Min J, Frenkel MB, Greenberg EJ, et al. Asiatic acid, a pentacyclic triterpene from Centella asiatica, is neuroprotective in a mouse model of focal cerebral ischemia. J Neurosci Res. 2009;87:2541–50.
49. Kim OT, Kim SH, Ohyama K, Muranaka T, Choi YE, Lee HY, et al. Upregulation of phytosterol and triterpene biosynthesis in Centella asiatica hairy roots overexpressed ginseng farnesyl diphosphate synthase. Plant Cell Rep. 2010;29:403–11.
50. Vanmierlo T, Weingärtner O, Pol S van der, Husche C, Kerksiek A, Friedrichs S, et al. Dietary intake of plant sterols stably increases plant sterol levels in the murine brain. J Lipid Res. 2012;53:726–35.
51. Saeed AA, Genové G, Li T, Hülshorst F, Betsholtz C, Björkhem I, et al. Increased flux of the plant sterols campesterol and sitosterol across a disrupted blood brain barrier. Steroids. 2015;99:183–8.
52. Cevatemre B, Botta B, Mori M, Berardozzi S, Ingallina C, Ulukaya E. The plant-derived triterpenoid tingenin B is a potent anticancer agent due to its cytotoxic activity on cancer stem cells of breast cancer in vitro. Chemico-Biological Interactions. 2016;260:248–55.
53. Hernndez L, Palazon J, Navarro-Oca A. The Pentacyclic Triterpenes alpha, beta-amyrins: A Review of Sources and Biological Activities. In: Rao V, editor. Phytochemicals - A Global Perspective of Their Role in Nutrition and Health. InTech; 2012. p. 491. doi:10.5772/27253.

54. Park SJ, Ahn YJ, Oh SR, Lee Y, Kwon G, Woo H, et al. Amyrin attenuates scopolamine-induced cognitive impairment in mice. Biol Pharm Bull. 2014;37:1207–13.
55. Alexander-Lindo RL, Morrison EYSA, Nair MG. Hypoglycaemic effect of stigmast-4-en-3-one and its corresponding alcohol from the bark of Anacardium occidentale (cashew). Phytother Res. 2004;18:403–7.
56. Vanella L, Di Giacomo C, Acquaviva R, Barbagallo I, Cardile V, Kim DH, et al. Apoptotic markers in a prostate cancer cell line: Effect of ellagic acid. Oncology Reports. 2013;30:2804–10.
57. Eskra JN, Schlicht MJ, Bosland MC. Effects of Black Raspberries and Their Ellagic Acid and Anthocyanin Constituents on Taxane Chemotherapy of Castration-Resistant Prostate Cancer Cells. Scientific Reports. 2019;9:4367.
58. Ahmed T, Setzer WN, Nabavi SF, Orhan IE, Braidy N, Nabavi ES-S and SM. Insights Into Effects of Ellagic Acid on the Nervous System: A Mini Review. Current Pharmaceutical Design. 2016. http://www.eurekaselect.com/138714/article. Accessed 5 Jun 2019.
59. Fisher N, Abd Majid R, Antoine T, Al-Helal M, Warman AJ, Johnson DJ, et al. Cytochrome b Mutation Y268S Conferring Atovaquone Resistance Phenotype in Malaria Parasite Results in Reduced Parasite bc1 Catalytic Turnover and Protein Expression. J Biol Chem. 2012;287:9731–41.
60. Ntie-Kang F, Zofou D, Babiaka SB, Meudom R, Scharfe M, Lifongo LL, et al. AfroDb: A Select Highly Potent and Diverse Natural Product Library from African Medicinal Plants. PLOS ONE. 2013;8:e78085.
61. ZINC95486072 | ZINC Is Not Commercial - A database of commercially-available compounds. http://zinc.docking.org/substance/95486072. Accessed 11 Jun 2019.
62. (9β,13α)-13,28-Epoxyoleanane-3,22-dione | C30H46O3 | ChemSpider. http://www.chemspider.com/Chemical-Structure.68899531.html?rid=84d90b9d-d6f7-4f21-a847-f08f132b209a. Accessed 11 Jun 2019.

Figures

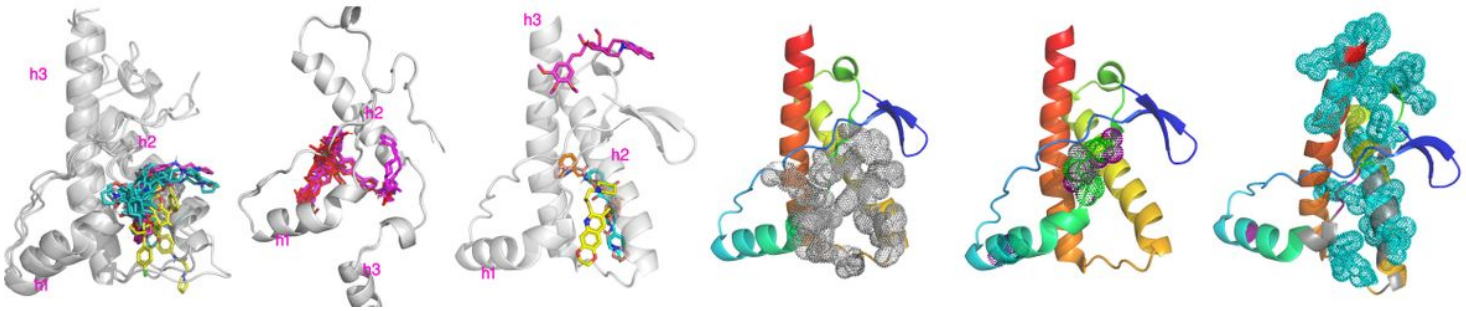

Figure 1

A: Binding regions of known and new compounds to the non-swapped (left), swapped (center) and non-swapped with ordered N-terminus structures. Compounds binding to different structures in the superimposed figures (left and center) are shown in different colors. B: Regions of prion protein showing regions of interaction. Swapped structures show binding with residues of α2-α 3 regions (left), residues of α 2 and α 3 facing each other as well as residues of α 1 (center) form interactions in the swapped structures, residues throughout α 2, α 2-α 3 switch regions as well as those of α 3 C-terminus (right) interact with compounds in the ordered N-terminus non-swapped structure. All regions are shown on the ordered N- terminus colored N- to C-terminus (blue to red) structure for comparison.

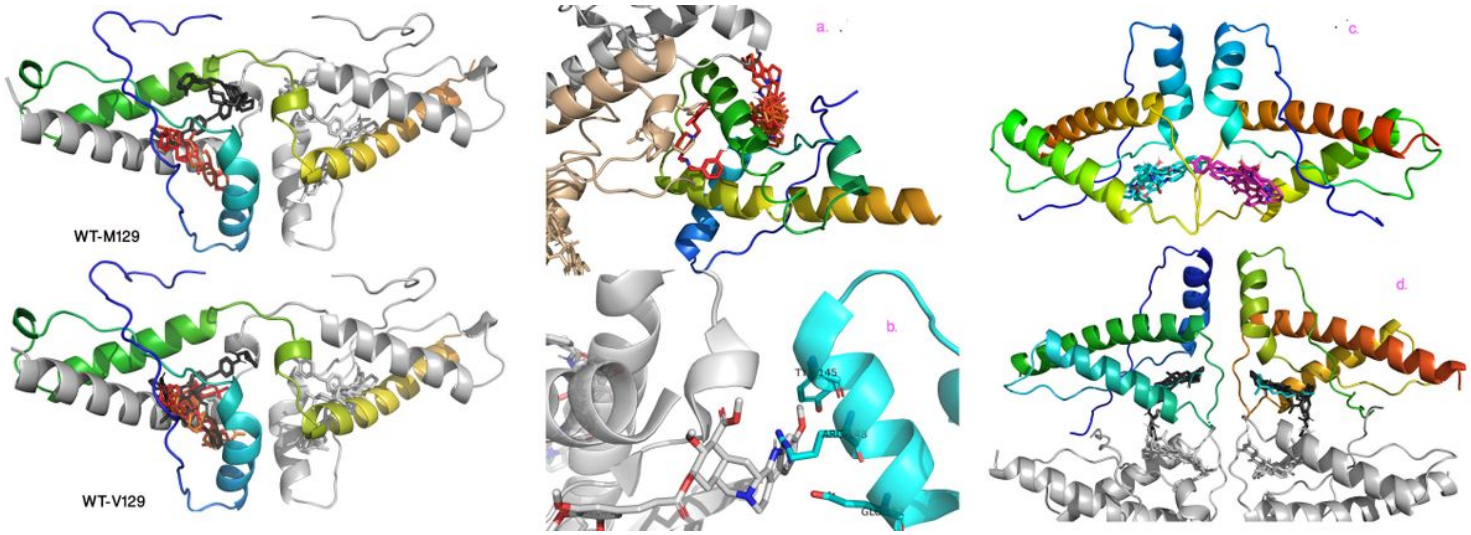

Figure 2

A: Swapped structure dimers (I4M top and HAF bottom) showing steric clashes of bound molecules bound between α1 and α2 of one monomer (blue to red) with the swapped α3 of the partner monomer (grey). Clashes are also seen with the residues of the switch region of the partner molecule. B: Steric clashes of bound compounds with partner monomers of the dimer and molecules related through crystallographic symmetry in the non-swapped structures. a. HAF showing steric clashes of compounds bound to one monomer (blue to red) with molecules related through crystallographic symmetry (grey and beige) b. Steric clash of RAU31 bound to the C-terminus of KML (grey) with residues of another molecule related through crystallographic symmetry (cyan) c. Steric clashes of bound compounds with each other in the dimer formed in HJX d. Two dimers of compound bound HEQ showing steric clashes with subunits of another dimer (grey) as well as compounds bound to them, but not with each other (blue to red)

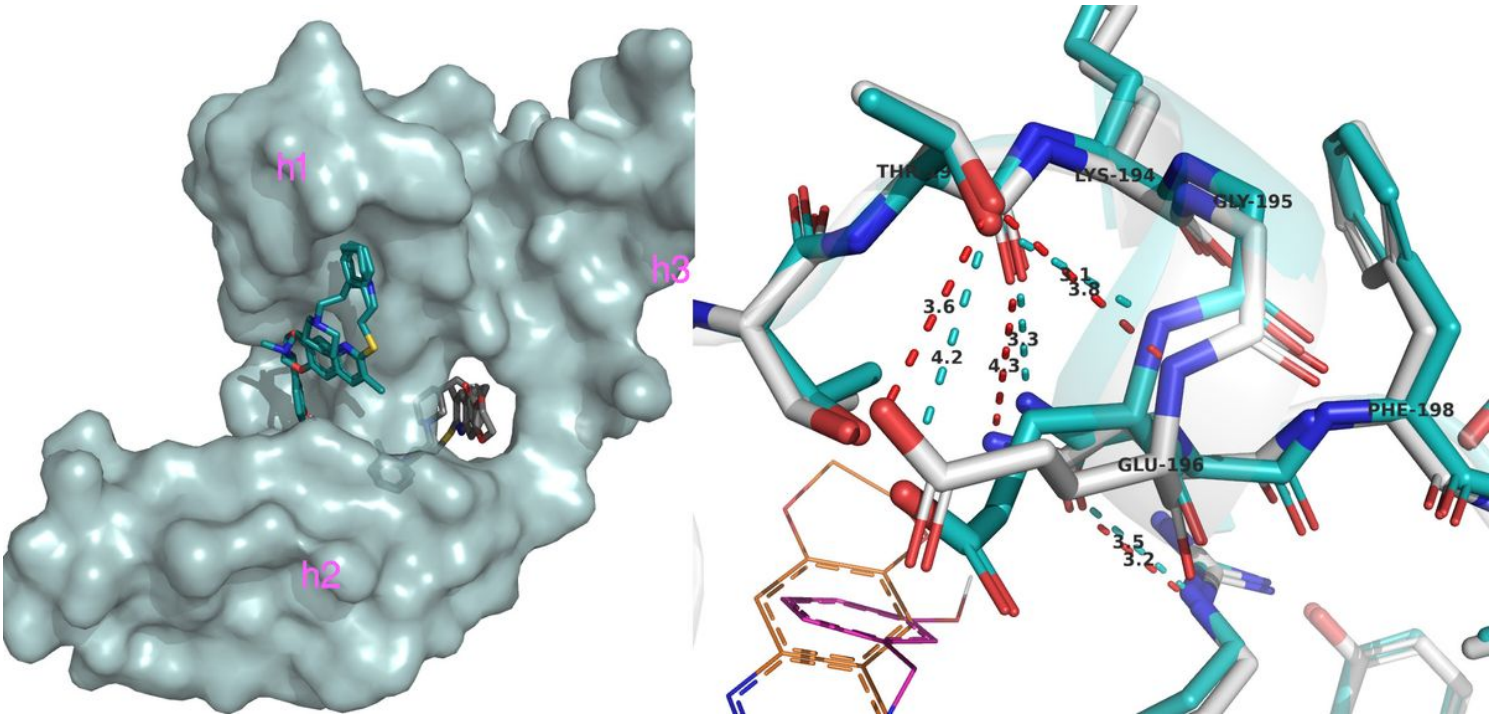

Figure 3

Differences in binding sites of LD7 and GJP49 to the swapped structures. Binding to HAF is on the surface (cyan) while to I4M is in the crevice (grey) (Left) when the only difference in the binding regions of either structure is a slight shift in side chain conformations of Glu196 and Asn197 (right) between I4M (grey) and HAF(cyan) so that ionic interactions with surrounding residues change (red I4M, cyan HAF).

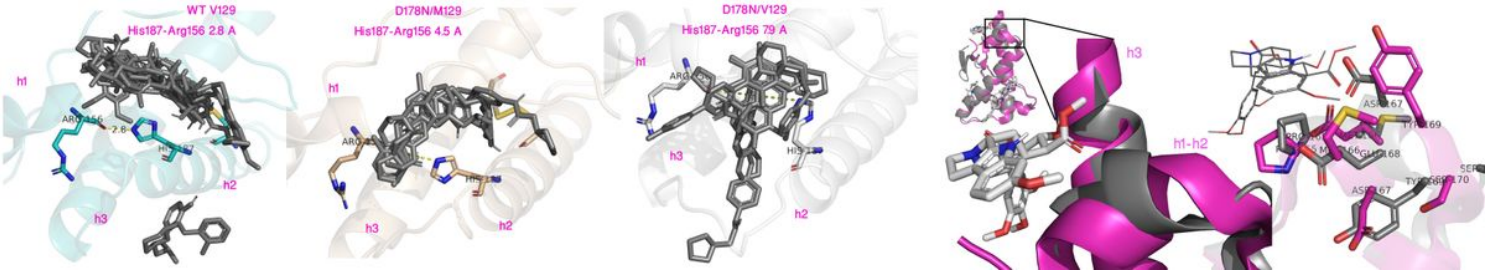

Figure 4

A: Distances between Arg156 of helix 1 and His 187 of helix 2 in the swapped structures that might determine access to binding of compounds. As h1 moves away, binding shifts towards the h2 –h3 loop Left:HAK, Center: HEQ, Right: HJX Figure 4B: Differences in binding of RAU31 to HAK(pink) and KML(grey) showing differences in the R164-S170 short helix region (left). Residues in this region are displaced in the two structures (right) and may be responsible for allowing RAU31 (shown in lines) to bind in KML while restricting it in HAK .

Supplementary Files

This is a list of supplementary files associated with this preprint. Click to download.

- SupplementaryMaterialS1.docx

- SupplementaryMaterialS2.docx